Q. J. R. Meteorol. Soc. (1996), **122**, pp. 1365–1383

Observation and simulation of barrier winds at the western margin of the Greenland ice sheet

By MICHIEL R. van den BROEKE[1]* and HUBERT GALLÉE[2]

[1] *Utrecht University, The Netherlands*

[2] *Université Catholique de Louvain, Belgium*

(Received 22 June 1995; revised 16 January 1996)

SUMMARY

Meteorological observations performed in the melting zone of the Greenland ice sheet during GIMEX-90/91 show the regular occurrence of moderately strong barrier-winds. The barrier wind is a thermally generated jet that develops when the large-scale flow advects warm tundra air towards the cold, melting ice sheet, creating a large local horizontal gradient of temperature. As a result, the geostrophic wind in the atmospheric boundary-layer acquires a component perpendicular to the temperature gradient. In the melting zone of the ice sheet, barrier winds interact with persistent surface-based katabatic winds. The forcing mechanisms and detailed two-dimensional structure of the barrier wind have been investigated with a mesoscale meteorological model. The model results confirm the important role of the warm tundra during the development of barrier winds. Barrier winds cause a pronounced rise in temperature and a strong increase of turbulent exchange in the lower melting zone: friction velocity and sensible-heat flux in the melting zone showed peak values of 1.3 m s^{-1} and 300 W m^{-2} respectively. In combination with large positive net radiation, the daily melt rate increased to 10 cm water equivalent, which is twice the rate in typical katabatic wind conditions. This shows that barrier winds could have a significant impact on the melt regime of areas where the ice sheet ends in the tundra. Although barrier winds in this part of Greenland may occur less frequently than the observations during GIMEX-90 suggest, they are of great importance for the climate of this and of other polar regions, such as the Antarctic, and so merit careful study.

KEYWORDS: Barrier winds Greenland ice sheet Ice-melting zone Mesoscale modelling

1. INTRODUCTION

The Greenland ice sheet stores enough water to increase global sea level by as much as 7.5 m (Oerlemans 1993). Each year, approximately 500 km^3 of water accumulates on the ice sheet in the form of snow. About half of this is lost by calving of icebergs, the other half by melting and run-off during the short arctic summer. The importance of surface melting and run-off for the mass balance makes the ice sheet quite sensitive to climate warming (Van de Wal and Oerlemans 1994). To increase our knowledge of the interaction between the atmospheric boundary-layer (ABL) and the mass balance of the ice sheet, the Greenland Ice Margin Experiment (GIMEX-90/91) was carried out near Søndre Strømfjord, in west Greenland, in the summers of 1990 and 1991.

Figure 1 gives a broad outline of the GIMEX arrangements. Temperature, humidity and wind were measured at a height of 6 m on several masts that were erected along a line crossing tundra (site WS, site 1 and base camp) and melting zone (sites 4, 5 and 6). WS denotes the Søndre Strømfjord weather station. Site 1 was placed at 5 km from the ice margin during GIMEX-90 (site 1-90), but was moved to a location closer to the ice margin in 1991 (site 1-91). Sites 4 and 5 are situated in the lower melting zone, site 6 in the higher melting zone. A tethered balloon was operated at the base camp (site BC) close to the ice margin. Characteristic of the expedition area—and more generally for the west coast of Greenland south of 73°N—is the wide strip of tundra between ice cap and sea. The tundra climate is generally dry and sunny, and the area near Søndre Strømfjord has the highest mean July temperature in Greenland (> +10 °C (Ohmura 1987)). The local orientation of the ice margin is approximately 330°/150°; 330° will be referred to as the

* Corresponding author: Norsk Polarinstitutt, Middelthunsgate 29, Postboks 5072 Majorstua, N 0301 Oslo, Norway.

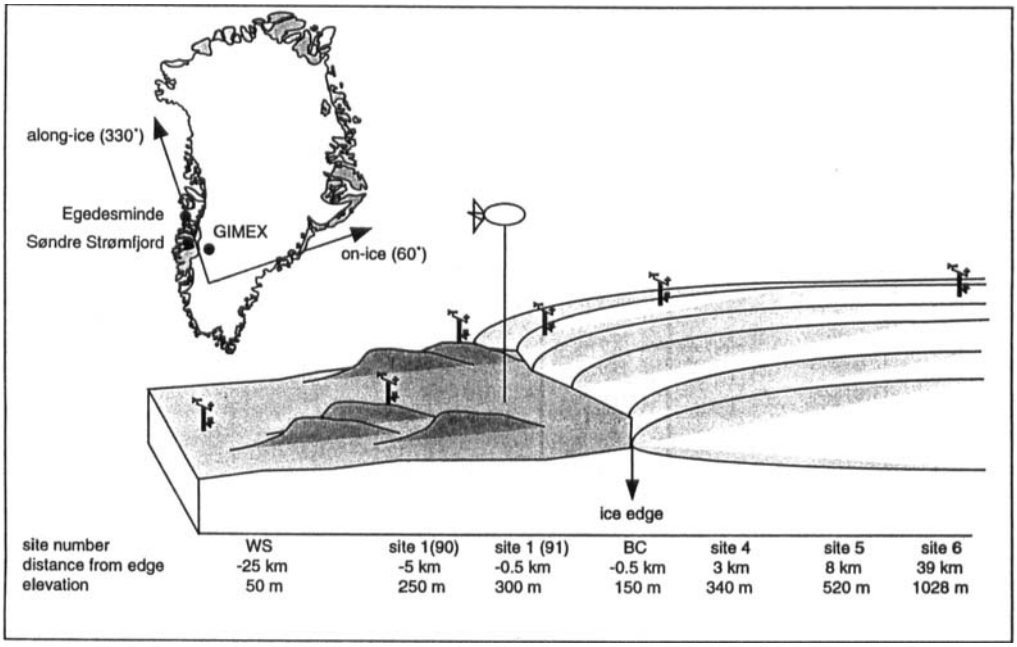

Figure 1. Experimental layout for GIMEX-90/91. The inset shows the location of Egedesminde, Søndre Strømfjord and the GIMEX area, as well as the direction of the on-ice and along-ice vectors. Note that site 1 was moved closer to the ice edge for the 1991 observations.

along-ice direction. Consequently, the on-ice direction is towards 060° (Fig. 1). For more details of the experiment see Oerlemans and Vugts (1993).

Especially during GIMEX-90, we frequently observed a low-level jet close to the ice margin that could not directly be associated with katabatic winds. This jet was identified as a barrier wind; it enhanced turbulent exchange and consequently increased the rate of melting substantially. Figure 2(a) illustrates the forcing mechanism schematically. Although the wind in the ABL is usually not in geostrophic balance, a discussion in terms of the geostrophic wind is the most convenient way to understand the formation of barrier winds. We will follow the lines set out by Schwerdtfeger (1975): during the summer, the ABL over west Greenland is cooled at the melting ice surface in the ablation zone (air is warmer than the surface) and heated over the tundra (surface warmer than the air). As a result, a horizontal gradient of temperature develops in the ABL perpendicular to the edge of the ice sheet. This gradient is steepest close to the surface and decreases with height above the ground. If the geostrophic wind at the top of the ABL (V_{g,h_b}) is directed from the ice sheet towards the tundra, the temperature gradient is decreased because the tundra surface adjusts its temperature to the cold air. When V_{g,h_b} has a component towards the ice, the temperature gradient will increase, because the surface of the melting ice cannot adjust its temperature to that of the warm air. In this case, the geostrophic flow within the ABL acquires a significant component v_T through the well known thermal-wind relation

$$\frac{\partial v_g}{\partial z} = \frac{g}{fT}\frac{\partial \theta}{\partial x}, \tag{1}$$

where θ is potential temperature, x the zonal coordinate perpendicular to the ice edge, f the Coriolis parameter and v_g the component of geostrophic wind parallel to the edge

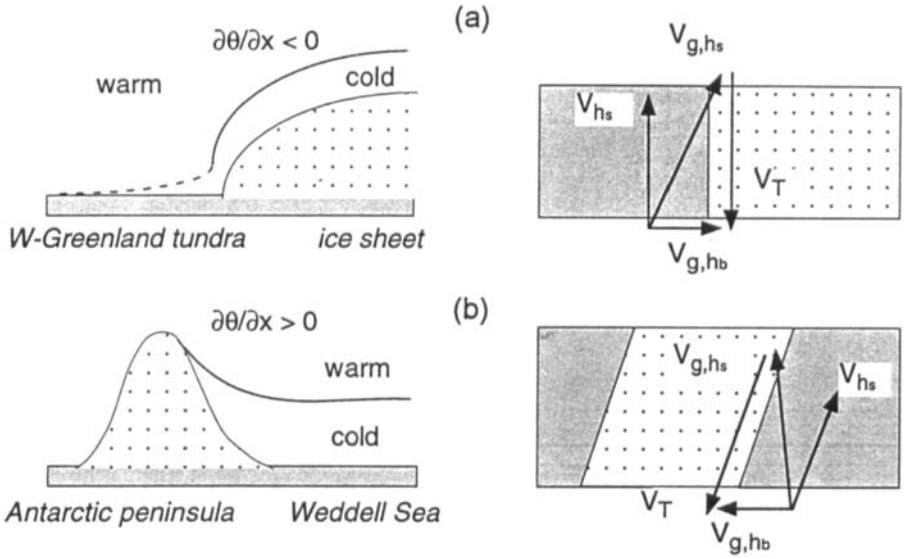

Figure 2. Schematic representation of the formation of barrier winds. For clarity, the ageostrophic component arising because of curved trajectories is omitted. V_{g,h_b} denotes the geostrophic wind vector at the top of the boundary layer, V_{g,h_s} the geostrophic flow at the surface, V_{h_s} the actual surface wind and V_T the vector thermal wind within the boundary layer. (a) At the western edge of the Greenland ice sheet in the area of Søndre Strømfjord; (b) along the Antarctic Peninsula on the east coast of the Weddell Sea (Schwerdtfeger 1975).

of the ice. For a typical, steep horizontal gradient of temperature close to the edge of the Greenland ice sheet, $\partial\theta/\partial x = 0.1$ K km^{-1}, we obtain a wind shear of 2.6 m s^{-1} per 100 m height increment! This results in a strong geostrophic wind at the surface V_{g,h_s} (Fig. 2(a)). When we include friction and a geostrophic turning of the wind caused by a topographic barrier, we obtain a near-surface wind V_{h_s} that is significantly stronger than would be expected given only the strength of the geostrophic flow above the ABL. It may be concluded that a jet blows in the ABL along the edge of the ice sheet. Hereafter, it is this jet which will be referred to as a barrier wind. The barrier wind is confined to the area with the strongest temperature gradient, which normally is the edge of the ice sheet, but it can be advected eastwards by the large-scale flow. That is why the effects of the jet (such as the downward mixing of warm air) can be quite pronounced at sites in the lower melting zone. In reality, the picture is somewhat more complicated than Fig. 2(a) suggests: very persistent surface-based katabatic winds blow down the fall line of the ice sheet in summer and obscure the presence of barrier winds aloft. The interaction of katabatic winds with barrier winds is one of the topics of this paper, and will be discussed in section 2.

Note that a topographic barrier is not necessarily needed to create a thermally forced circulation at the edge of the ice sheet. (Compare the ice-breeze circulation at the edge of snow patches (Segal *et al.* 1991).) However, a topographic barrier enhances the ageostrophic turning of the wind and furthermore prevents the advection of cold air far onto the ice. So, in this paper, we shall retain the name 'barrier winds' because of the similar forcing mechanisms involved. Local winds produced by the presence of a barrier occur elsewhere. Persistent surface winds (without the presence of local heat sources or sinks such as occur in Greenland) are observed in the western Weddell Sea in the Antarctic, for example (Schwerdtfeger 1975). These are illustrated schematically in Fig. 2(b). They occur when cold, strongly stratified air from the Filchner–Ronne ice shelf is advected towards the

mountains of the Antarctic Peninsula, where low-level convergence on the upwind side exceeds upper-level divergence (the so-called 'piling up' of cold air) and a horizontal gradient of temperature is created. It is interesting to note that this 'cold' type of barrier wind could also occur in Greenland during the winter when cold, stratified air is often present over the snow-covered tundra. Simulations with mesoscale models of this type of barrier winds were performed by Parish *et al.* (1993) and H. Gallée, P. Pettré and G. Schlayes (personal communication).

In the present paper we shall discuss observations of barrier winds in Greenland. With the aid of synoptic charts and upper-wind data, we investigate which large-scale pressure distribution favours the development of barrier winds in west Greenland. To do so, three near-surface flow types are defined for the melting zone of the Greenland ice sheet: 'barrier/katabatic', 'pure katabatic' and 'weak katabatic'. In a study of well-developed barrier-winds (22–26 July 1990), a mesoscale meteorological model is used to simulate the observed barrier-winds in order to refine our understanding of the forcing mechanisms involved. In section 5 we discuss the impact that barrier winds have on the observed ice-melt rates in the lower melting zone.

2. Classification of flow types during GIMEX

With the aid of surface synoptic charts and GIMEX data, we introduce a classification of the summertime flow over the melting zone of the Greenland ice sheet. A convenient way to classify gravity flows is to identify the most important terms in the momentum budget (Mahrt 1982). For convenience, we look at the vertically integrated momentum-equation for turbulent boundary-layer flow over a sloping surface:

$$\underset{\text{term}}{\phantom{\frac{\mathrm{d}U}{\mathrm{d}t}}} \qquad \underset{\text{I}}{\phantom{\frac{1}{D}\frac{\partial(0.5\Delta_\theta D^2)}{\partial x}}} \qquad \underset{\text{II}}{\phantom{+\Delta_\theta\frac{\partial h_s}{\partial x}}} \qquad \underset{\text{III}}{} \quad \underset{\text{IV}}{} \qquad \underset{\text{V}}{\phantom{\frac{w_e\Delta u+(\overline{u'w'})_{h_s}}{D}}}$$

$$\frac{\mathrm{d}U}{\mathrm{d}t} = \frac{g}{\theta_r}\left\{\frac{1}{D}\frac{\partial(0.5\Delta_\theta D^2)}{\partial x} + \Delta_\theta\frac{\partial h_s}{\partial x}\right\} + f(V - v_g) + \left\{\frac{w_e\Delta u + (\overline{u'w'})_{h_s}}{D}\right\} \quad (2)$$

where the subscript 'r' denotes a reference value, the x-coordinate points in the downslope direction, h_s is surface elevation, U is the characteristic speed of the down-slope wind, V the characteristic speed of the cross-slope wind. D is the characteristic depth of the boundary layer, Δ_θ the potential temperature deficit of the boundary layer compared to the background potential temperature, w_e the entrainment velocity at the top of the ABL, Δu the velocity difference across the ABL top and f the Coriolis parameter. The different terms in the momentum-budget equation represent: (I) *thermal-wind* arising from horizontal gradients in density and ABL thickness. Forces represented by this term drive the ice- or sea-breeze circulation over flat terrain and are primarily responsible for barrier winds, if the time scale is sufficiently long to establish a coupling via the Coriolis force; (II) *katabatic or buoyancy* force arising from the presence of an inversion layer over sloping terrain. During an average summer in Greenland, all areas below the −10 °C July isotherm (2500–3000 m a.s.l.) experience one or more melt days (Ohmura 1987). Because the melting surface can no longer increase its temperature, a surface-based temperature inversion develops which, in combination with the sloping surface, generates persistent katabatic winds; (III) the *Coriolis force*; (IV) *synoptic pressure-gradient* above the boundary layer, which includes effects of the mesoscale gradients of temperature in the lower troposphere; (V) *frictional dissipation* at the surface and top of the ABL.

Three circulation patterns and their associated flow types within the ABL over the melting zone could be defined during GIMEX (Fig. 3):

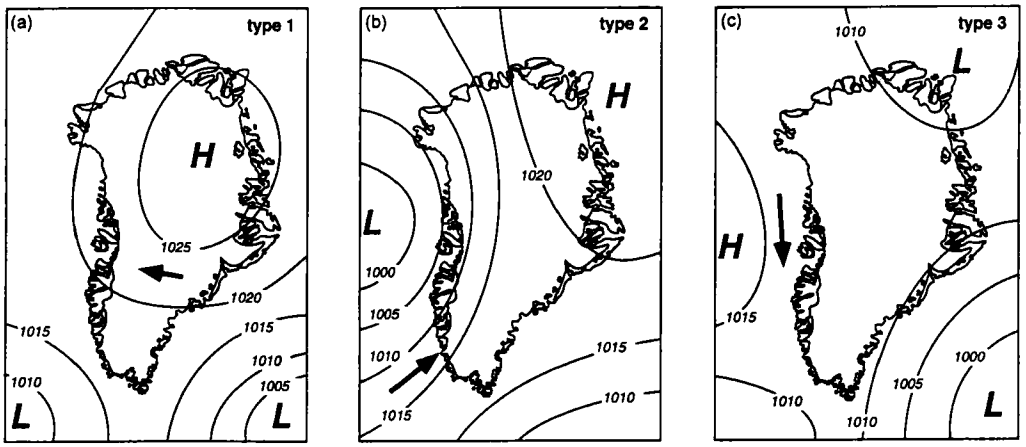

Figure 3. Typical distributions of surface pressure for three types of flow. See text for details. (a) Flow type 1, purely katabatic; (b) flow type 2, barrier/katabatic; (c) flow type 3, weak katabatic.

Flow type 1 (pure katabatic): high pressure prevails over the ice sheet and areas of low pressure pass south of Cape Farewell (Fig. 3(a)). This is probably the most frequently observed pressure-distribution in the Greenland area (Scorer 1988; Putnins 1970). The geostrophic flow in the area of Søndre Strømfjord is weak and directed off the ice sheet. Conditions over the tundra are sunny and relatively warm, but the advection of cold air from the ice limits the horizontal temperature-gradient between the tundra and the melting zone. The flow over the melting zone is purely katabatic (i.e. not significantly influenced by the large-scale circulation), deflected from the topographic fall-line by the Coriolis force: term II shows a generation of down-slope momentum which is balanced by terms III and V. Term I is unimportant when we look at daily mean values, although on shorter timescales it imposes a daily cycle on the flow close to the edge of the ice (ice-breeze mechanism). At site 4, because of the steep slope of the ice surface, we observe almost pure down-slope or antitriptic flow (balance between terms II and V). This type of flow is similar to katabatic winds observed in the Antarctic (Ball 1960; Weller 1969; Wendler and Kodama 1985). The daily cycle and the momentum, heat and moisture budgets of pure katabatic flow in Greenland have been described in more detail by van den Broeke *et al.* (1994a, b).

Flow type 2 (barrier/katabatic): the high pressure area has moved to the north-east, clearing the way for a low pressure area that approaches Greenland from the west (Fig. 3(b)). In the study area, warm tundra air is advected towards the ice sheet by relatively strong south-westerly large-scale winds. Barrier winds will gradually develop in the presence of a marked temperature contrast between the tundra and the ice sheet. In combination with the south-westerly synoptic winds above the ABL and katabatic winds at the surface, we observe strong near-surface winds in the melting zone. The advection of warm air also tends to enhance the katabatic component, so all terms I to V are probably important for this flow type.

Flow type 3 (weak katabatic): advection of relatively cold and cloudy air from northern regions to the study area reduces possible differences in the temperature of the air over the tundra and of that over the ice sheet: both are around 0 °C, so that thermal-wind effects will be small (Fig. 3(c)). Unless the temperature of the advected air at the surface is below 0 °C, weak katabatic winds prevail above the melting zone. They are modified by the synoptic flow and by frictional forces (balance between terms II, IV and V). During summer it is

unlikely that the advected air will be cold, or stratified, enough to generate barrier winds of the Antarctic type (Fig. 2(b)).

3. Observations of barrier winds

For the present study we use data from the periods 18 July to 17 August 1990 and 10 June to 24 July 1991. The 850 hPa wind measured at Egedesminde (a coastal station 250 km farther to the north, see Fig. 1) is considered to be representative of the large-scale flow above the boundary layer in the GIMEX area. We decomposed the 850 hPa vector wind into on-ice (060°) and along-ice (330°) components, taking into account the orientation of the ice margin on a regional scale (Fig. 1). A positive/negative value of u_{850} indicates that the synoptic-scale flow is directed towards/off the ice sheet. In the present study we use data for 78 days. To remove some scatter from the graphs, we present 3-day running means in this section.

(*a*) *Flow types during GIMEX-91*

Figure 4 shows the wind components at 850 hPa and values of the wind speed and direction and potential temperature near the surface at various sites during GIMEX-91. One barrier-wind signature is visible during this experiment, from 22 to 26 June (indicated by the *B* in Fig. 4(d)). During this period, the 850 hPa flow had a significant on-ice component (Fig. 4(a)); results from the masts close to the ice edge show a gradual increase in wind speed from the south (Fig. 4(b)). No significant increase in wind speed is observed farther from the edge of the ice at site WS. The increase in wind speed between site 4 and site 6 suggests that the jet was advected onto the ice by the large-scale flow. The wind direction becomes south-east at site 1 (Fig. 4(c)). Although the change of the wind direction at the ice-sheet stations is not so pronounced (because of the strong katabatic component) a general turning to the south is clearly visible. A clear barrier-wind signature is found in the temperature record at site 4, where during barrier-wind conditions the temperature at 2 m shows a significant rise. Because the near-surface wind direction remains directed off the ice as a result of the persistent katabatic winds near the surface (Fig. 4(c)), this significant temperature rise (Fig. 4(d)) must be a result of enhanced downward mixing of warm tundra air rather than horizontal advection from the tundra. In general, the formation of a low-level jet with high wind-speeds above the melting zone of the ice sheet will create a deep turbulent layer, which mixes potentially warm air down to the surface. This warm air will, in combination with strong winds, increase surface melt. This is the subject of section 5 of this paper.

On 27 June the ambient air cooled in response to northerly synoptic-scale flow that advected cold air to the study area. The thermal contrast between tundra and ice sheet vanished, and the barrier winds ceased (Fig. 4(b)). We see a gradual transition towards type 3 flow with low wind-speeds and low temperatures. Before 21 June 1991 and after 5 July 1991, high pressure dominated the flow over the ice sheet for several weeks (type 1). The 850 hPa wind at Egedesminde was generally weak and directed off the ice. The large input of solar radiation strongly warmed the tundra ABL. The near-surface winds over the ice sheet were of a katabatic nature, influenced by the rotation of the earth: the wind direction was 120° at site 6, almost down slope at site 4 and north-east over the tundra, which is the direction of the main topographic features that channel the cold outflow. Note that barrier winds started to develop around July 15, but the on-ice directed geostrophic flow was apparently too weak to build up sufficient temperature-contrast at the edge of the ice sheet. The potential-temperature record shows a minimum at site 4, indicating that the ABL air constantly cooled as it flowed down the ice sheet. Long periods of type 1

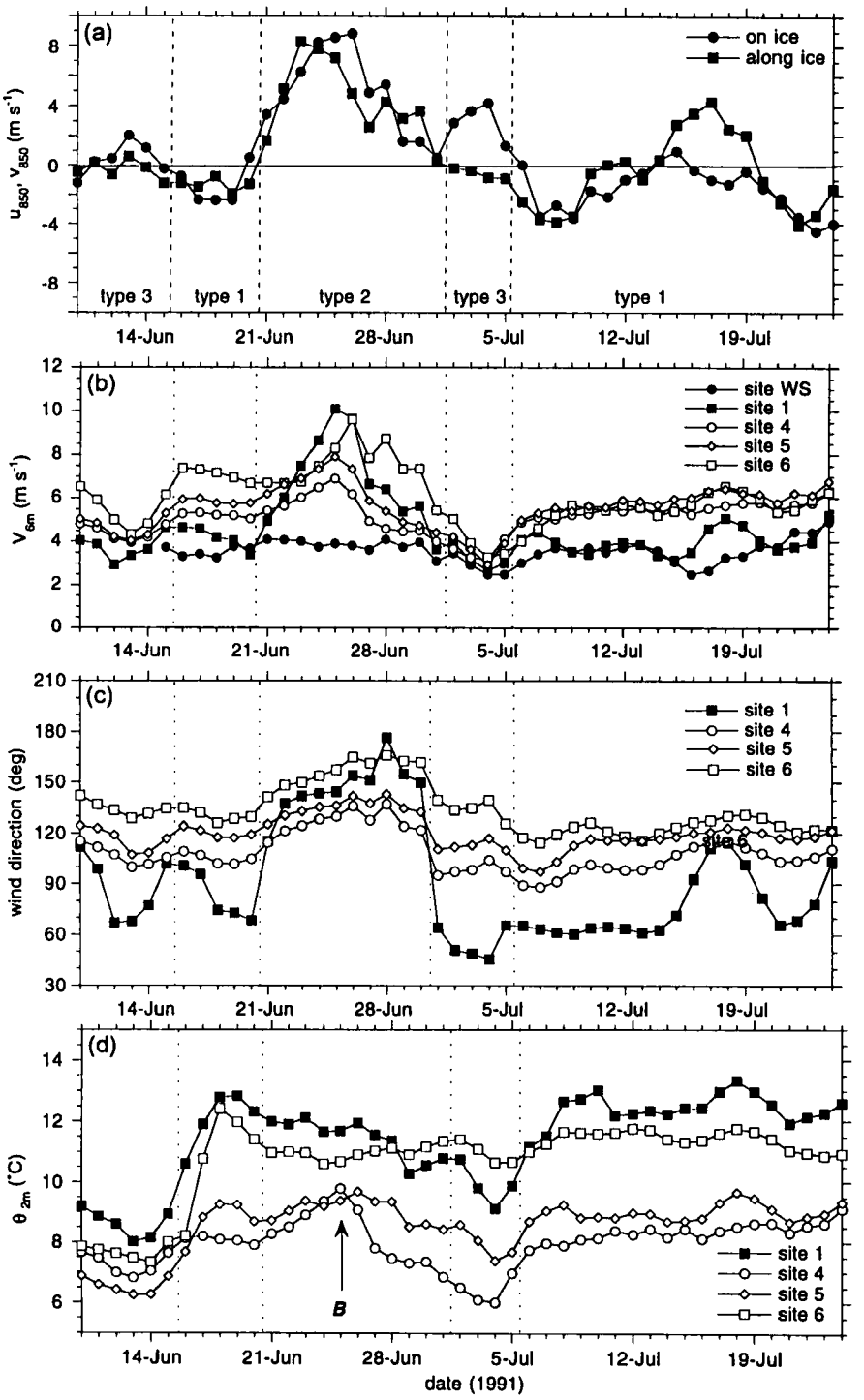

Figure 4. 3-day running means during GIMEX-91. See text for further details. (a) On-ice and along-ice components of the flow at 12 UTC, at 850 hPa, above Egedesminde. Associated flow types are shown at the bottom. (b) Wind speed at a height of 6 m at five sites. (c) wind direction at a height of 6 m at four of the five sites used for (b). (d) Potential temperature at 2 m at the four sites used for (c)—the *B* indicates a barrier-wind signature.

flow are probably representative of Greenland katabatic winds in summer, and have been described by Van den Broeke *et al.* (1994a, b) and Duynkerke and Van den Broeke (1994). Modelling studies of this period have been made by Meesters *et al.* (1994) and Gallée *et al.* (1995).

(*b*) *Flow types during GIMEX-90*

During GIMEX-90, synoptic-scale activity was stronger than during GIMEX-91, and the large-scale flow had a more pronounced on-ice component (Fig. 5). Clearly, this had implications for the near-surface flow over the melting zone, which showed the regular development of barrier winds (indicated by *B*'s in Fig. 5(d)). Especially in the period 22–26 July 1990, barrier winds were very well developed. During this period, the jet was close to the edge of the ice; note the high wind-speed at site 1-90 and at site 4 and the lower wind-speed at site 6. The air temperature at 2 m increased over the tundra and over the entire melting zone. In the subsequent two periods with barrier winds, the highest wind-speeds were observed on the ice at site 6. Because of the smaller gradient of temperature between the tundra and the ice (Fig. 5(d)), these barrier winds are not very well developed. This can be attributed to the decreasing strength of solar radiation towards the end of the summer season and the consequent general cooling in the northern hemisphere.

Several balloon-soundings were performed at BC during moderately strong barrier-wind conditions on 24 July 1990. In Fig. 6, vertical profiles of wind speed, wind direction and potential temperature obtained on 24 July 1990 may be compared with profiles that are representative of purely katabatic flow a few days earlier (type 1, 19 July 1990). The profiles clearly demonstrate the jet structure of the barrier wind and the interaction with the shallow but persistent katabatic winds in the lowest layers of the atmosphere. During barrier-wind conditions, the air in the ABL is 4 or 5 K warmer than when katabatic winds advect cold air from the ice sheet. This illustrates the strengthening of the horizontal gradient of temperature near the edge of the ice during barrier-wind conditions. The increased stability in the lowest 500 m (Fig. 6(c)) is a result of the persistent katabatic winds that bring cold air towards the tundra, and is not representative of advected tundra air, which is unstable. This will be shown in the next section.

4. Simulation of barrier winds with a two-dimensional mesoscale model

In order to refine our understanding of barrier winds in west central Greenland during summer, two idealized simulations of the atmospheric circulation in this area have been created using the two-dimensional version of the hydrostatic primitive equation model MAR (Modèle Atmosphérique Regional, e.g. Gallée and Schayes 1994). The model, model-domain and discretization (i.e. $\Delta x = 5$ km, 17 vertical levels) are those used by Gallée *et al.* (1995), except that the topography of the lower boundary was specified as level tundra at a height of 0 m a.s.l. The initial vertical profile of potential temperature (K) is $\theta_0 = 283.15 + 4z$ where z is the altitude (in km). Experiment 1 was made with an on-ice large-scale wind of 8 m s^{-1} while in experiment 2 a calm large-scale wind was prescribed. The large-scale situation of experiment 1 comes very close to that observed on 24 July 1990, when barrier winds were observed near the ice-sheet margin (Fig. 5). In experiment 2 the large-scale flow was set to zero; it was conducted in order to compare the barrier/katabatic type of flow with the more frequent purely katabatic type of flow prevailing in this region. The main results for the third simulated day are shown in Table 1.

In experiment 1, strong southerly barrier-winds were simulated at mast 4 (i.e. near the edge of the ice sheet), in quantitative agreement with the observations. A good agreement is also found at mast 6, where the observed and simulated barrier-winds are less strong.

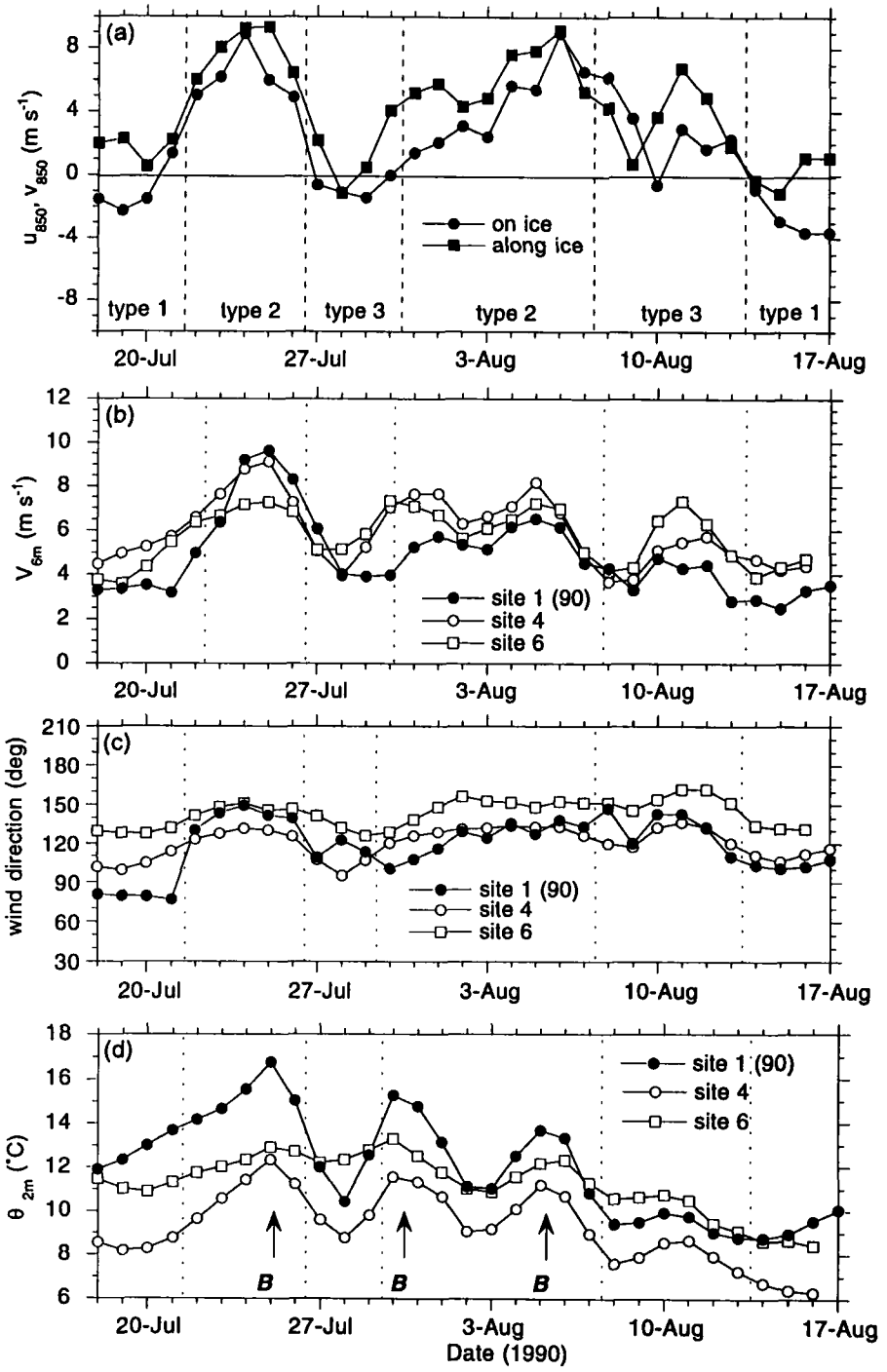

Figure 5. As Fig. 4, but for GIMEX-90 and for three sites in (b), (c) and (d).

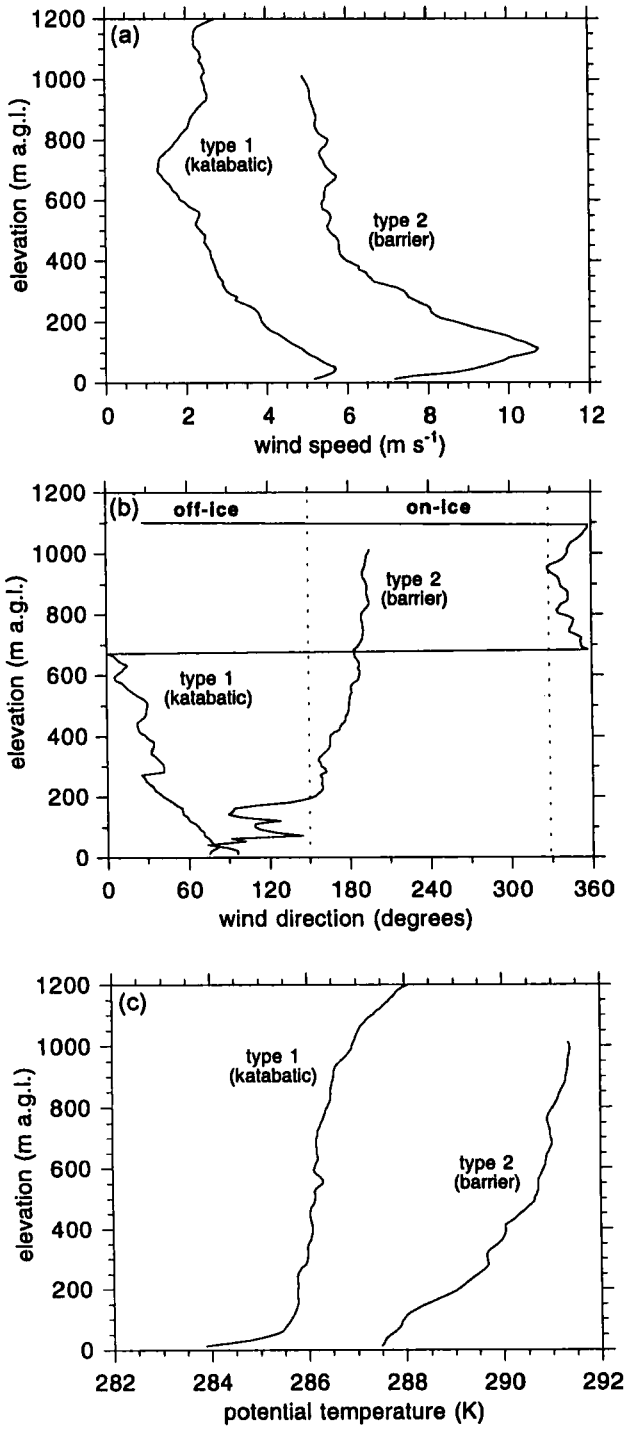

Figure 6. Observed profiles, based on radio soundings made at site BC, at 12 UTC on 19 July 1990 (flow type 1, katabatic) and 24 July 1990 (flow type 2, barrier): (a) wind speed; (b) wind direction—on-ice and off-ice sectors are shown by dotted lines; (c) potential temperature.

TABLE 1. SIMULATIONS OF THE CIRCULATION OF THE ATMOSPHERE IN CENTRAL WEST GREENLAND ON 24 JULY 1990

Experiment number	u_g, v_g (m s^{-1})	Site 1			Site 4			Site 6		
		u (m s^{-1})	v (m s^{-1})	H (W m^{-2})	u (m s^{-1})	v (m s^{-1})	H (W m^{-2})	u (m s^{-1})	v (m s^{-1})	H (W m^{-2})
1	(8, 0)	−1.5	5.8	−111	−3.2	9.6	89.8	−1.1	6.6	1
2	(0, 0)	−2.4	0.9	−112	−6.2	1.5	52.6	−2.1	0.9	10

Daily average of simulated wind 6 m above the surface and sensible-heat flux H (positive downward), for the third day of integration at grid points 58, 59 and 66, corresponding to site 1 (located on the tundra, 5 km from the edge of the ice sheet) and sites 4 and 6 (located on the ice sheet, 2.2 and 29 km from the edge of the ice sheet respectively). (u_g, v_g) is the prescribed large-scale forcing at the coast. u denotes a component of the flow directed towards the ice and v a component blowing parallel to the edge of the ice. Negative values of u indicate katabatic flow and positive values of v indicate a southerly wind.

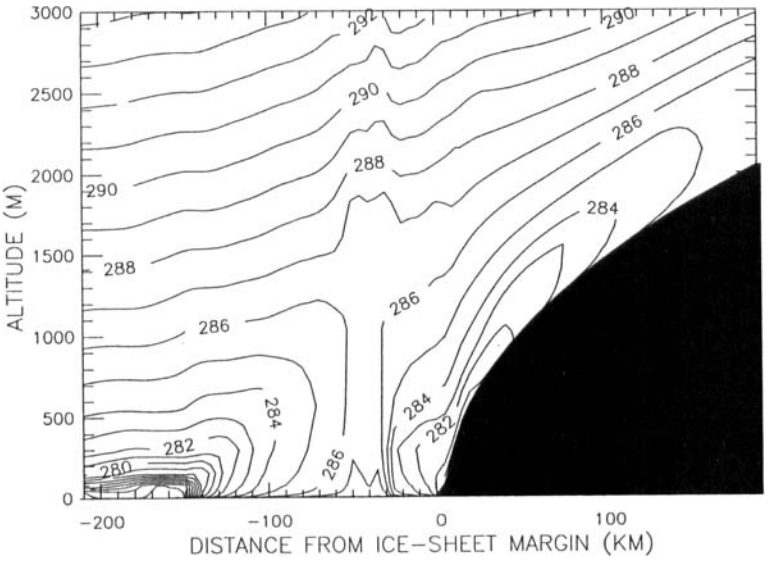

Figure 7. Vertical section normal to the ice edge after 63 simulated hours (i.e. at 15 h (= 12 UTC) 24 July 1990), from experiment 1 of the two-dimensional mesoscale model simulations. See section 4 of text for details. Potential temperature; contour interval 1 K.

Such agreement indicates that the horizontal extent of summer barrier-winds over the west Greenland ice sheet is simulated well by the model. Agreement is fair at site 1, if we take into account that this mast was situated on a hill top at an elevation of 250 m a.s.l., while the model assumes a flat tundra.

The fields of potential temperature and of the components of down- and cross-slope winds for experiment 1 are presented in Figs. 7 and 8 respectively. These figures confirm that a marked difference exists between summer barrier-winds over west Greenland and winter barrier-winds near the Antarctic Peninsula (Fig. 2). This is explained as follows: in west Greenland, the area near the ice sheet is warm tundra, so that the boundary layer over it is warm and unstable; consequently, no cold air from the tundra is available for piling up at the foot of the ice sheet; this is in contrast to what happens near the Antarctic Peninsula, where cold air forms over the cold Filchner–Ronne ice shelf and is then piled up against the mountains of the peninsula (e.g. Parish 1983). Such a difference suggests

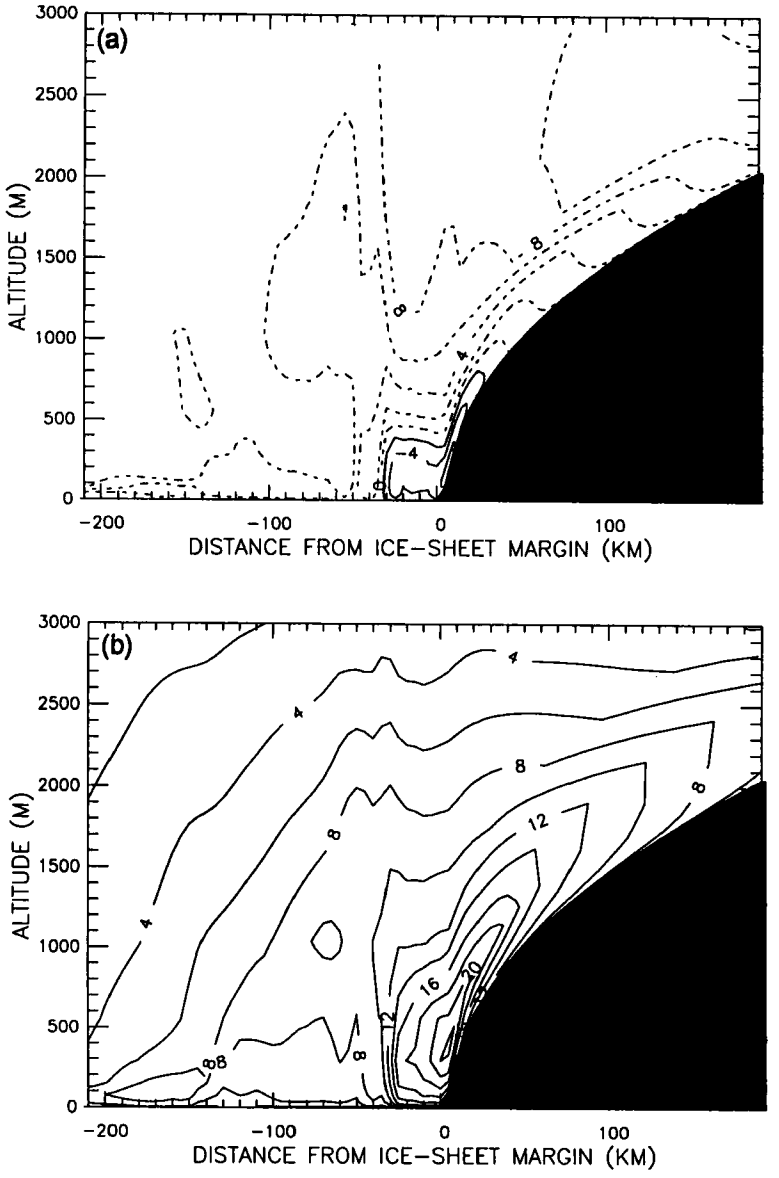

Figure 8. As Fig. 7 but for orthogonal components of the wind field: contour interval 2 m s^{-1}. (a) On-ice component u; negative values (full lines) denote a down-slope wind. (b) Along-slope component v; all values are positive, denoting the component from a direction of 150°, parallel to the local direction of the ice edge.

that summer barrier-winds over west Greenland do not result from a simple piling up of cold air originating from the flat area surrounding the ice sheet. The apparently stable stratification of the tundra air close to the ice margin, as shown in Fig. 6(c), is a direct consequence of the advection of cold ice-sheet air in the lower part of the ABL by the persistent katabatic flow. Farther away from the edge of the ice, the tundra air is unstable (Fig. 7).

On the basis of experiments conducted with a two-dimensional mesoscale model, Meesters (1994) suggested that strong southerly winds over west Greenland result from

the counteraction of the warm eastward wind above the tundra and the cold glacier-wind. An examination of Experiment 1 results allows a better understanding of this mechanism. Looking at the simulated fields of potential temperature and horizontal wind for 15 h local time (= UTC − 3 hours) (Figs. 7 and 8), it is seen that (i) cold air is simulated in the boundary layer over the ice sheet; this pool of cold air is limited seawards by the unstable boundary-layer over the tundra; (ii) a relatively weak although significant katabatic circulation is simulated in the pool of cold air near the edge of the ice sheet; note that this katabatic flow is maintained against a relatively strong on-ice large-scale wind (8 m s^{-1}) and that the katabatic wind speed amounts to roughly 50% of simulated purely katabatic flows (Table 1); (iii) strong barrier-winds are simulated almost exclusively in the pool of cold air. It appears that strong downward sensible-heat fluxes H are responsible for a substantial cooling of the boundary layer near the ice-sheet margin. (At site 4, the daily average of H is 89.8 W m^{-2}, almost twice the value for simulated purely katabatic winds.) The consequence of this cooling is the maintenance of the stable stratification which disconnects the boundary layer from the large-scale airflow and allows the development of a katabatic circulation over the ice sheet slopes (e.g. van den Broeke and Bintanja 1995). In turn, the katabatic circulation maintains the pool of cold air near the edge of the ice sheet, generating a steep horizontal gradient of temperature between the cold boundary-layer over the ice sheet and the warm boundary-layer over the tundra. Finally, barrier winds develop at low levels.

Strong fluxes of sensible heat at site 4 occur because the temperature of the surface in this area is at the melting point whereas that of the air is much higher and the wind is strong. The interaction between the strong sensible-heat flux, the katabatic flow and the strong barrier winds may be viewed as a mechanism for positive feedback, in which each process reinforces the others. In the model output, the katabatic airflow stops suddenly over the tundra. As a result, a sharp transition forms between off-ice katabatic flow and on-ice large-scale winds, at a relatively small distance from the edge of the ice-sheet. The sharp transition may occur because, over the tundra, the katabatic air is strongly heated from below, so that its stratification becomes rapidly unstable, subsequently reconnecting the katabatic layer with the overlying atmosphere. In short, the process described here resembles the mechanism described by Schwerdtfeger (1975), except that the 'cold' air generation is activated by strong sensible-heat losses to the surface of the ice sheet that is maintained at the 'cold' melting point, and 'warm' air generation is fed by the convective boundary-layer over the tundra.

5. The impact of barrier winds on the energy balance at site 4

In order to quantify the influence of barrier winds on the melt rate in the lower melting zone, we calculated the energy balance from observations made at site 4 for an 11-day period (18 to 28 July 1990) that contained the three different types of flow. The energy balance for a surface of melting ice or snow is

$$M = Shw_{in}(1 - \alpha) + (Lw_{in} - 315) + H + LE + G, \qquad [\mathrm{W\ m^{-2}}] \qquad (3)$$

where M is the melting energy, Shw_{in} is the incoming solar or shortwave radiation, α the surface albedo, Lw_{in} the incoming terrestrial or longwave radiation, H the turbulent flux of sensible heat and LE the turbulent flux of latent heat. Terms are positive when directed towards the surface. The sub-surface heat flux G is generally small in the melting zone (Ambach 1977) and will be neglected here. The short-wave radiation balance was measured directly, while Lw_{in} was estimated using the parametrization proposed by Konzelmann *et*

al. (1994). 315 W m^{-2} is the long-wave radiation lost by the melting ice surface. To calculate the turbulent fluxes of sensible heat H and latent heat LE, we used Monin–Obukhov similarity theory. This relates the scales of turbulent fluctuations of momentum u^*, heat θ^* and moisture q^* in the surface layer to the surface fluxes through

$$H = \rho c_p(\overline{w'\theta'})_{h_s} \cong \rho c_p u^* \theta^* \tag{4}$$

$$LE = \rho L_v(\overline{w'q'})_{h_{hs}} \cong \rho L_v u^* q^*, \tag{5}$$

where ρ is the air density, c_p the specific heat of air at constant pressure and L_v the latent heat of vaporization. These scales are calculated using the approach of Munro (1989), see appendix.

First we will discuss how the turbulent scales at site 4 varied with time (Fig. 9). During katabatic wind conditions (18 to 21 July 1990), u^* reflects the pronounced daily cycle of the wind speed at site 4 (Fig. 9(a)). θ^* shows minor diurnal variation during flow type 1 while q^* is small and slowly decreases, probably because of advection of dry air from the ice sheet (Fig. 9(b),(c)). When barrier winds developed in the period following 22 July 1990, u^*, θ^* and q^* increased steadily, because of the increasing near-surface wind speed and the downward mixing of warm, humid air originating from the tundra. In the period with barrier winds (22 to 26 July), u^* averaged 0.83 m s^{-1}, which is 59% more than in flow type 1; θ^* increased on average by 36%, to a value of 0.15 K. On July 26, friction velocity u^* peaked at 1.3 m s^{-1} and θ^* at 0.22 K. When the temperature contrast between the tundra and the ice sheet vanished on 27 July, the barrier winds ceased abruptly. A sharp transition towards flow type 3 occurred, with weak katabatic winds and a sudden decrease of turbulent exchange in the surface layer.

Of course, the evolution of the turbulent scales has important implications for the turbulent fluxes (Fig. 10). The sensible-heat flux H increases strongly from 65 W m^{-2} during flow type 1 to values between 100 and 300 W m^{-2} during flow type 2. The latent-heat flux, being small during katabatic flow conditions (5 W m^{-2}) reaches values up to 50 W m^{-2} during barrier-wind conditions. These values are extremely high for the stable boundary-layer. As shown in the appendix, the surface layer is only moderately stable, because wind speeds are high, and the surface of the ice is aerodynamically rough. If we add the radiation components to the fluxes, we can use Eq. (3) to calculate the melt rate at site 4, and compare it with the observed melt. Integrated over the period 22 July (15 h) to 26 July (15 h) the calculated melt equals 34.1 cm water equivalent (w.e.), which compares favourably with the observed value of 36.3 cm w.e. for the same period. This indicates that the energy-balance components are calculated/measured with sufficient accuracy. The calculated melt-rate (Fig. 11) shows a pronounced increase from 4 or 5 cm w.e. day^{-1} during flow type 1 to 6–10 cm w.e. day^{-1} during barrier-wind conditions (flow type 2), which is entirely the result of increased fluxes of sensible and latent heat.

6. Discussion and conclusions

As shown in section 5, barrier winds can cause very high melting rates in areas where the ice sheet ends in the tundra. Turbulence generated by these winds effectively mixes down the warm tundra-air to the ice surface. Model results confirm that, in west Greenland, barrier winds are caused by the presence of warm tundra-air close to the 'cold' melting ice. However, it is still not clear how frequently barrier winds occur. From the GIMEX data set, obtained in just a few summer months, this question cannot be answered with any certainty. At most, we may conclude that the circulations in the two years were different, with frequent barrier-winds in 1990 and only one in 1991. Few studies of the

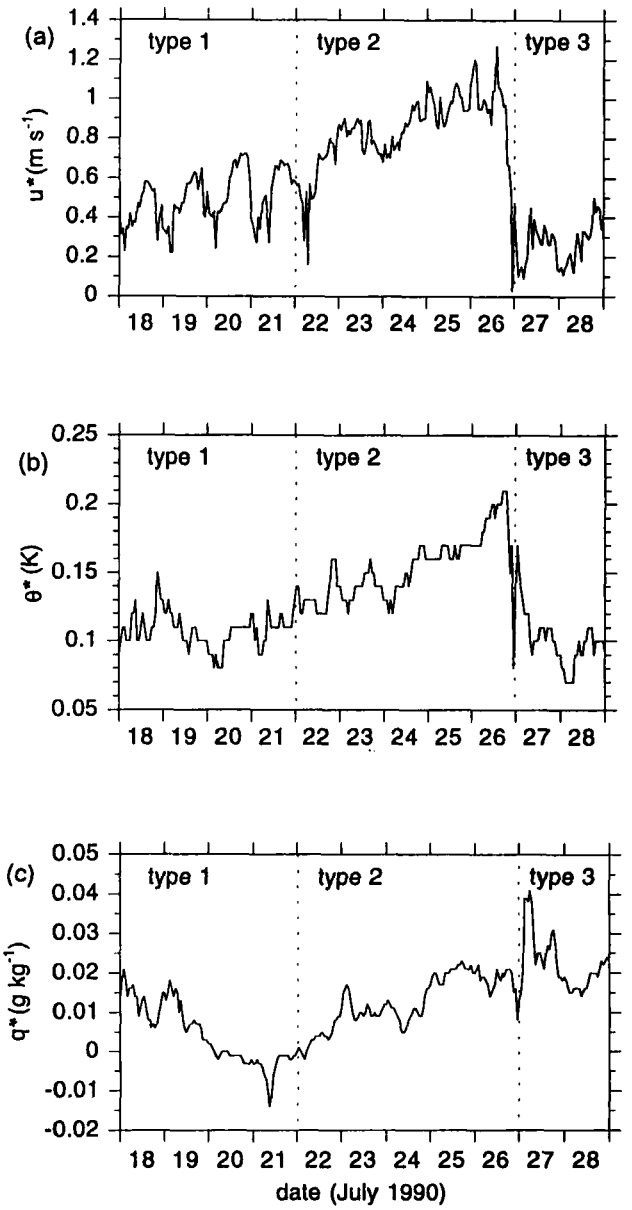

Figure 9. Hourly mean values of three quantities derived from observations at site 4, for the period 18 to 28 July 1990, during all three types of flow: (a) u^*; (b) θ^*; (c) q^*.

synoptic circulation over a longer period are available. Putnins (1970) states that areas of low pressure quite frequently move north along the west coast of Greenland, where they sometimes intensify. This suggests that westerly, large-scale winds directed towards the ice are common in west Greenland. On the other hand, statistics of upper-wind data at Egedesminde show a very small zonal component at 850 and 700 hPa. An analysis of surface-wind data by Hedegaard (1982) proves that meteorological stations along the west coast, including Søndre Strømfjord, seldom experience westerly winds. Scorer (1988) agrees; he states that areas of low pressure generally do not move north into the Davis

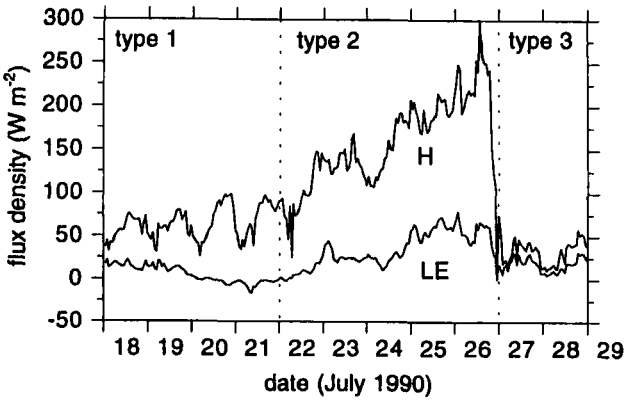

Figure 10. Hourly mean values (W m^{-2}) of the turbulent flux of sensible heat H and of latent heat LE, derived from measurements made at site 4 during the period from 18 to 28 July 1990, during all three types of flow.

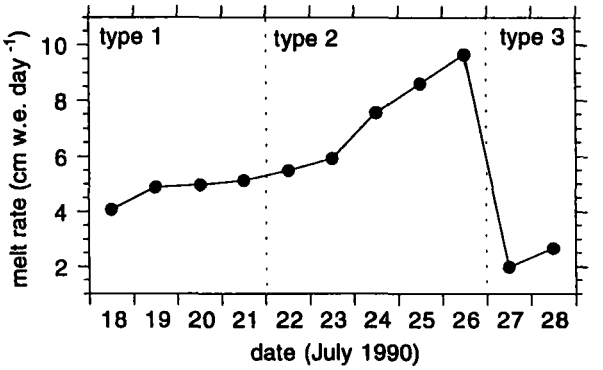

Figure 11. Calculated daily melt rates (cm of water equivalent per day) at site 4 for the period from 18 to 28 July 1990, during all three types of flow.

Strait. He writes: "The impression sometimes given of significant depressions passing up the west coast (of Greenland) was not confirmed by satellite pictures since 1977, and the west winds across the coast that they might cause are very rare." From the foregoing, we might conclude that barrier-wind conditions do not occur frequently. Data from automatic weather-stations in the marginal zone of the Greenland ice sheet will soon provide a more solid answer to this question.

Acknowledgements

All members of the GIMEX expeditions, as well as the staff of the Søndre Strømfjord meteorological office, are thanked for support. Peter G. Duynkerke, Hans Oerlemans and two anonymous reviewers are thanked for remarks that significantly improved the manuscript. Financial support was obtained from the Dutch National Research Programme on Global Air Pollution and Climate Change (contract 276/91-NOP) and from the Commission of the European Communities (contracts EPOC-CT90-0015 and EV5V-CT92-0132). Hubert Gallée is supported by the Belgian Scientific Research Program on the Antarctic, of the Prime Minister's Science Policy Office.

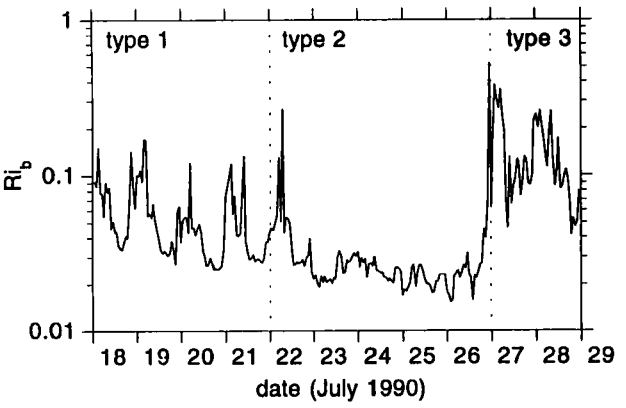

Figure A.1. Calculated bulk Richardson number Ri_b on a logarithmic scale, for the period from 18 to 28 July 1990, during all three types of flow.

Appendix

Calculation of the surface fluxes

Munro (1989) used a bulk method to calculate H and LE above a melting glacier with good results, and in this paper we have followed his approach. We use hourly mean values of wind speed, temperature and humidity at 6 m and assume that the melting ice surface remains at 0 °C, while the air just above it is saturated with respect to water. A value of 12 cm is adopted for the aerodynamic roughness length z_0, based on the microtopographical formula presented by Lettau (1969) and closure of the energy balance (Van den Broeke 1996). The roughness length for heat and moisture z_h is determined using the expression proposed by Andreas (1987). This expression relates z_h to z_0 as a function of the roughness Reynolds number $Re = u^* z_0 \nu^{-1}$, where ν is the kinematic viscosity of air. Data collected by Bintanja and Van den Broeke (1995a), Munro (1989) and Kondo and Yamazawa (1986) confirmed the general shape of Andreas's expression for a wide range of roughness Reynolds numbers (Bintanja and van de Broeke 1995b). The stability corrections given by Duynkerke (1991) are used; for moderately stable conditions ($zL^{-1} \ll 1$) these expressions yield good results, and are quite similar to those proposed by Högström (1987). To study the stability of the surface layer, we use the bulk Richardson number Ri_b, calculated from the surface to 6 m (Fig. A.1):

$$Ri_b = \frac{g/\theta_r(\theta_6 - \theta_s)(z - z_0)^2}{V_6^2(z - z_h)}. \tag{A.1}$$

During flow type 2, the mechanical generation of turbulence by katabatic/barrier winds is strong enough to overcome the thermal stratification of the surface layer, given the small values of Ri_b. By contrast, type 3 flow is characterized by weak winds, large Ri_b and weak turbulent exchange between atmosphere and ice sheet. During flow type 2, the strong daily cycle of the katabatic wind is reflected in the daily cycle of the surface-layer stability: very stable at night, but only moderately stable during most of the day. For all flow types, Ri_b remains below the critical value of 1; so, judging from the present data, the surface layer is expected to be continuously turbulent, in spite of strong thermal stratification.

References

Ambach, W. 1977 Untersuchungen zum Energieumsatz in der Ablationszone des Grönländische Inlandeises. *Expedition Glaciologique Internationale au Groenland*, **4**, No. 5, Bianco Lunos Bogtrykkeri A/S, Copenhagen

Andreas, E. L. 1987 A theory for the scalar roughness and the scalar transfer coefficients over snow and sea ice. *Boundary-Layer Meteorol.*, **38**, 159–184

Ball, F. K. 1960 'Winds on the ice slopes of Artarctica'. Pp. 9–16 in *Antarctic Meteorology: proceedings of the symposium, Melbourne 1959*, Pergamon, New York

Bintanja, R. and van den Broeke, M. R. 1995a The surface energy balance of Antarctic snow and blue ice. *J. Appl. Meteorol.*, **34**, 902–926

1995b Momentum and scalar transfer coefficients over aerodynamically smooth Antarctic surfaces. *Boundary-Layer Meteorol.*, **74**, 89–111

Duynkerke, P. G. 1991 Radiation fog: a comparison of model simulation with detailed observations. *Mon. Weather Rev.*, **119**, 324–341

Duynkerke, P. G. and van den Broeke, M. R. 1994 Surface energy balance and katabatic flow over glacier and tundra during GIMEX-91. *Global Planet. Change*, **9**, 17–28

Gallée, H. and Schayes, G. 1994 Development of a three-dimensional meso-γ primitive equations model: katabatic winds simulation in the area of Terra Nova Bay, Antarctica. *Mon. Weather Rev.*, **122**, 671–685

Gallée, H., de Ghélin, O. F. and van den Broeke, M. R. 1995 Simulation of atmospheric circulation during the GIMEX-91 experiment using a meso-γ primitive equations model. *J. Climate*, **11**, 2843–2859

Hedegaard, K. 1982 'Wind vector and extreme wind statistics in Greeland'. Weather Service Report No. 1, Danish Meteorological Institute, Copenhagen

Högström, U. 1987 Non-dimensional wind and temperature profiles in the atmospheric surface layer: A re-evaluation. *Boundary-Layer Meteorol.*, **42**, 55–78

Kondo, J. and Yamazawa, H. 1986 Bulk transfer coefficient over a snow surface. *Boundary-Layer Meteorol.*, **34**, 123–135

Konzelmann, T., van de Wal, R. S. W., Greuell, W., Bintanja, R., Henneken, E. A. C. and Abe-Ouchi, A. 1994 Parametrization of global and longwave incoming radiation for the Greenland ice sheet. *Global Planet, Change*, **9**, 143–164

Lettau, H. H. 1969 Note on aerodynamic roughness parameter estimation on the basis of roughness element description. *J. Appl. Meteorol.*, **8**, 828–832

Mahrt, L. 1982 Momentum balance of gravity flow, *J. Atmos. Sci.*, **39**, 2701–2711

Meesters, A. G. C. A. 1994 Dependence of the energy balance of the Greenland ice sheet on climate change: influence of katabatic wind and tundra. *Q. J. R. Meteorol. Soc.*, **120**, 491–517

Meesters, A. G. C. A., Henneken, E. A. C., Bink, N. J., Vugts, H. F. and Cannemeyer, F. 1994 Simulation of the atmospheric circulation near the Greenland ice sheet margin. *Global Planet. Change*, **9**, 53–68

Munro, D. S. 1989 Surface roughness and bulk heat transfer on a glacier: Comparison with eddy correlation. *J. Glaciol.*, **35**, 343–348

Oerlemans, J. 1993 Possible changes in the mass balance of the Greenland and Antarctic ice sheets and their effects on sea level. Warrick, Barrow, Wigley (eds.): *Climate and sea level change*, Cambridge, U.K.

Oerlemans, J. and Vugts, H. F. 1993 A meteorological experiment in the melting zone of the Greenland ice sheet. *Bull. Am. Meteorol. Soc.*, **74**, 355–365

Ohmura, A. 1987 New temperature distribution maps for Greenland. *Z. Gletscherkd. Glazialgeol.*, **23**, 1–45

Parish, T. R. 1983 The influence of the Antarctic Peninsula on the wind field over the western Weddell Sea. *J. Geophys. Res.*, **88**, 2684–2692

Parish, T. R., Pettré, P. and Wendler, G. 1993 The influence of large-scale forcing on the katabatic wind regime at Adélie Land, Antarctica. *Meteorol. Atmos. Phys.*, **51**, 165–176

Putnins, P.	1970	The climate of Greenland. S. Orvig (ed.), *World Survey of Climatology, vol. 17: the climate of the polar regions*. Elsevier, Amsterdam
Schwerdtfeger, W.	1975	The effect of the Antarctic peninsula on the temperature regime of the Weddell Sea. *Mon. Weather Rev.*, **103**, 45–51
Scorer, R. S.	1988	Sunny Greenland. *Q. J. R. Meteorol. Soc.*, **114**, 3–29
Segal, M., Garratt, J. R., Pielke, R. A. and Ye, Z.	1991	Scaling and numerical model evaluation of snow-cover effects on the generation and modification of daytime mesoscale circulations. *J. Atmos. Sci.*, **48**, 1024–1042
Van den Broeke, M. R.	1996	Characteristics of the lower ablation zone of the west Greenland ice sheet for energy-balance modelling. *Ann. Glaciol.*, accepted
Van den Broeke, M. R. and Bintanja, R.	1995	Summertime atmospheric circulation in the vicinity of a blue ice area in Queen Maud Land, Antarctica. *Boundary-Layer Meteorol.*, **72**, 411–438
Van den Broeke, M. R., Duynkerke, P. G. and Henneken, E. A. C.	1994a	Heat, momentum and moisture budgets of the katabatic layer over the melting zone of the West-Greenland ice sheet in summer. *Boundary-Layer Meteorol.*, **71**, 393–413
Van den Broeke, M. R., Duynkerke, P. G. and Oerlemans, J.	1994b	The observed katabatic flow at the edge of the Greenland ice sheet during GIMEX-91. *Global Planet. Change*, **9**, 3–15
Van de Wal, R. S. W. and Oerlemans, J.	1994	An energy balance model for the Greenland ice sheet. *Global Planet. Change*, **9**, 115–132
Weller, G.	1969	A meridional wind speed profile in Mc Robertson Land, Antarctica. *Pure Appl. Geophys.*, **77**, 193–200
Wendler, G. N. and Kodama, Y.	1985	Some results of climatic investigations in Adélie Land, Eastern Antarctica. *Z. Gletscherkd. Glazialgeol.*, **21**, 319–3217